Available online at www.sciencedirect.com

ScienceDirect

Journal of the European Ceramic Society 32 (2012) 1435–1439

www.elsevier.com/locate/jeurceramsoc

ZrB_2–SiC laminated ceramic composites

Zhihui Lü [a,b], Dongliang Jiang [a,*], Jingxian Zhang [a], Qingling Lin [a], Zhengren Huang [a]

[a] *State Key Laboratory of High Performance Ceramics and Superfine Microstructures, Shanghai Institute of Ceramics, Chinese Academy of Sciences, Shanghai 200050, PR China*

[b] *Graduate University of the Chinese Academy of Sciences, Beijing 100049, PR China*

Abstract

The oxidation behavior for ZrB_2–20 vol% SiC (ZS20) and ZrB_2–30 vol% SiC (ZS30) ceramics at 1500 °C was evaluated by weight gain measurements and cross-sectional microstructure analysis. Based on the oxidation results, laminated ZrB_2–30 vol% SiC (ZS30)/ZrB_2–25 vol% SiC (ZS25)/ZrB_2–30 vol% SiC (ZS30) symmetric structure with ZS30 as the outer layer were prepared. The influence of thermal residual stress and the layer thickness ratio of outer and inner layer on the mechanical properties of ZS30/ZS25/ZS30 composites were studied. It was found that higher surface compressive stress resulted in higher flexural strength. The fracture toughness of ZS30/ZS25/ZS30 laminates was found to reach to 10.73 MPa $m^{1/2}$ at the layer thickness ratio of 0.5, which was almost 2 times that of ZS30 monolithic ceramics.

Keywords: ZrB_2–SiC; Mechanical properties; Laminated ceramic composites

1. Introduction

Ultra-high temperature ceramics (UHTCs) are a family of materials including several diborides, carbides and nitrides of the group IVB and VB transition metals, for example, ZrB_2, HfB_2, TaC, ZrC, HfC and HfN.[1] The interest in UHTCs has increased significantly in recent years[2–4] due to their remarkable properties of high melting point, high thermal conductivities, good oxidation resistance, and excellent corrosion resistance.[5–7] These properties make them promising candidates for high temperature structural applications, including long time hypersonic flight, rocket propulsion system, leading edge and nose cap, molten metal crucible, etc.

Among the UHTCs, ZrB_2 is of particular interest due to its lower theoretical density (6.09 g/cm^3) and lower cost, which can be advantages over other candidates for aerospace applications. It has been proved that the addition of SiC could not only improve the sinterability of ZrB_2 ceramics,[8,9] but also increased the oxidation resistance and mechanical properties of ZrB_2 ceramics,[10–13] Therefore, a lot of research works have been carried out on ZrB_2–SiC composites.

However, despite their attractive properties and potential applications, the preparation of the ZrB_2–SiC materials with tailored microstructure and synergistic properties, such as improved reliability, high thermal shock resistance, etc. is still a challenge for their application in severe environments. Ceramic composites with multilayered structures have been considered one of the possible route for improving the brittleness[14] and thermal shock behavior.[15]

In our previous research, ZrB_2–SiC sheets with different compositions were prepared by aqueous tape casting. After lamination and hot pressing, the microstructure and mechanical properties of the monolithic ZrB_2–SiC ceramics were characterized.[16] In the present study, the oxidation behavior of monolithic ZrB_2–SiC ceramics was investigated. Based on the results, laminated ZrB_2–SiC ceramics with composition and structure control were prepared and the mechanical properties were characterized.

2. Experimental procedure

Commercially available ZrB_2 powders (average particle size ~3.2 μm, oxygen content 3.0 wt%, Dandong Chemical Engineering Institute Co. Ltd., China) and SiC powders (0.31 μm, α-phase, FCP 15C, Sika Tech., Norway) were used as raw materials. ZrB_2–SiC composites were named as ZS (for ZrB_2 and SiC) along with the SiC content (based on total ceramic powder). For example, the ceramic prepared from ZrB_2 and 20 vol% SiC was named as ZS20.

---

[*] Corresponding author. Tel.: +86 21 5241 2606; fax: +86 21 5241 3122.
E-mail address: dljiang@sunm.shcnc.ac.cn (D. Jiang).

0955-2219/$ – see front matter © 2011 Elsevier Ltd. All rights reserved.
doi:10.1016/j.jeurceramsoc.2011.04.020

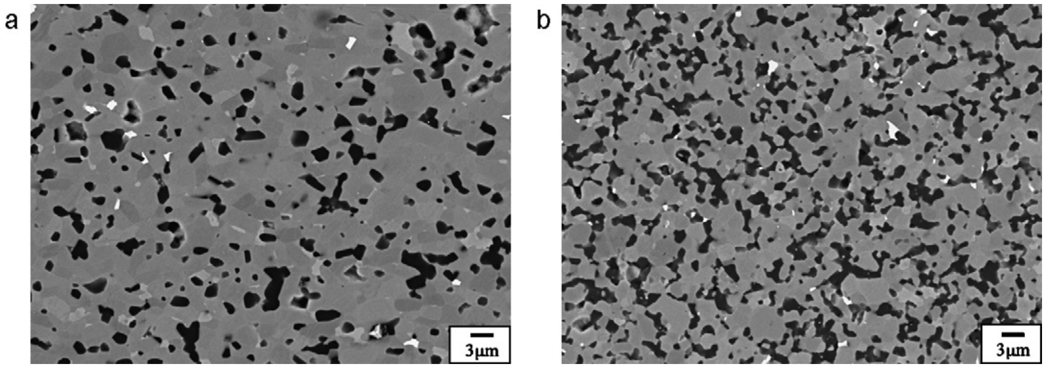

Fig. 1. SEM micrographs of the polished surfaces of (a) ZS20 and (b) ZS30.

The as-received ZrB_2 powder was attrition milled for 2 h at 300 rpm in water using WC as the media followed by acid treatment. The details of the processing have been reported previously.[17] Aqueous ZrB_2–SiC slurries were prepared by mixing as-treated ZrB_2 powder, SiC powder and dispersant into dionized water. Slurries were ball milled with zirconia media for 24 h, followed by adding emulsion binder and plasticizer. Then the slurries were ball milled for another 12 h. After homogenization, the slurries were degassed under vacuum to remove air bubbles. Finally, tape casting was performed on Procast Precision Tape Casting Equipment (HED International, Inc., USA) with a gap height of 400 μm at a speed of 100 mm/min. The shear rate was calculated to be $\sim 4\ s^{-1}$. After drying freely in open air at ambient temperature for 4–5 h, green tapes were obtained. The green tapes were laminated and heat treated at 500 °C for 1 h to remove the binder. Then, the pyrolysed samples were sintered at 1900 °C for 45 min under an applied pressure of 32 MPa in Ar atmosphere.[18]

The densities of the sintered ceramics were measured using Archimedes method with water as the immersing media, respectively. Flexural strength was tested in three-point bending on 3 mm × 4 mm × 36 mm bars, using a span width of 30 mm and a crosshead speed of 0.5 mm/min (Model 5566, Instron Corp.). Fracture toughness was measured by a single-edge notched beam test with a span of 16 mm and a crosshead speed of 0.05 mm/min using 2 mm × 4 mm × 22 mm test bars, on the same jig used for the flexural strength. Specimens with dimensions of 3 mm × 4 mm × 36 mm were used for oxidation behavior study after polishing. Prior to oxidation, specimens were cleaned in an ultrasonic bath with acetone. Then the specimens were placed on alumina plates and heated to 1500 °C at a rate of 10 °C/min in stagnant air (HT 40/17; Nabertherm Gmbh, Lilienthal, Germany). The microstructure of the sintered ceramics and oxidized specimens was observed by scanning electron microscopy (JXA 8100, Jeol, Tokyo, Japan) with energy-dispersive spectroscopy (EDS).

3. Results and discussion

The oxidized surface layer of SiC particles could react with the oxides on ZrB_2 surface,[8,9] and the remove of the oxides from ZrB_2 would allow the densification process occur more easily. The relative densities of the as-sintered ZS20 and ZS30 ceramics were 99.2% and 99.6%, respectively. Thus, the low porosity was considered to be ineffective for the consequent oxidation behavior tests. Fig. 1 showed the surface microstructure of ZS20 and ZS30 ceramics. No obvious porosity was found on the surface, which was in agreement with the density measurements. The black SiC phase dispersed homogeneously in the grey ZrB_2 matrix. Besides ZrB_2 and SiC phases, the SEM images revealed the presence of a brighter WC phase, which was probably introduced during attrition milling.[18] Previous reports demonstrated that the flexural strength of ZrB_2–SiC ceramics were controlled by the size of SiC grains rather than the size of ZrB_2 grain.[19,20] When SiC content increased from 20 vol% to 30 vol%, the SiC particles in the matrix tended to aggregate and therefore formed larger SiC agglomerates,[21] which would resulted in a decrease in flexural strength and fracture toughness.[16]

The main oxidation reactions of ZrB_2–SiC ceramics at 1500 °C could be described as follows[22,23]:

$$ZrB_2(s) + \tfrac{5}{2}O_2(g) \rightarrow ZrO_2(s) + B_2O_3(l) \quad (1)$$

$$B_2O_3(l) \rightarrow B_2O_3(g) \quad (2)$$

$$SiC(s) + \tfrac{3}{2}O_2(g) \rightarrow SiO_2(l) + CO(g) \quad (3)$$

The molten SiO_2 formed on the surface of ZrB_2–SiC ceramics would provide effective barrier to oxygen diffusion, resulting in passive oxidation protection with parabolic weight gain kinetics. The weight gain versus oxidation time at 1500 °C for ZS20 and ZS30 ceramics was shown in Fig. 2. The weight gain curves of ZS20 and ZS30 ceramics both illustrated parabolic weight gain kinetics, while the weight gain of ZS20 ceramic was higher than that of ZS30 ceramics with the same oxidation time. After being oxidized at 1500 °C for 10 h, the weight gain of ZS20 ceramic was 7.55 mg/cm^2, but that of ZS30 ceramic was 6.59 mg/cm^2.

Fig. 3 showed the cross-sectional microstructure of ZS20 and ZS30 ceramics after oxidized at 1500 °C for 10 h. The linear element distribution results were inserted at the top right corner of the micrographs. For both ceramics, the cross-sectional layered structure consisted of: (I) a silica-rich glassy layer; (II) a porous ZrO_2 layer; (III) unaffected ZrB_2–SiC ceramics. The thickness of layers I and layer II was 28 μm and 58 μm respectively for ZS20 ceramics but was 27 μm and

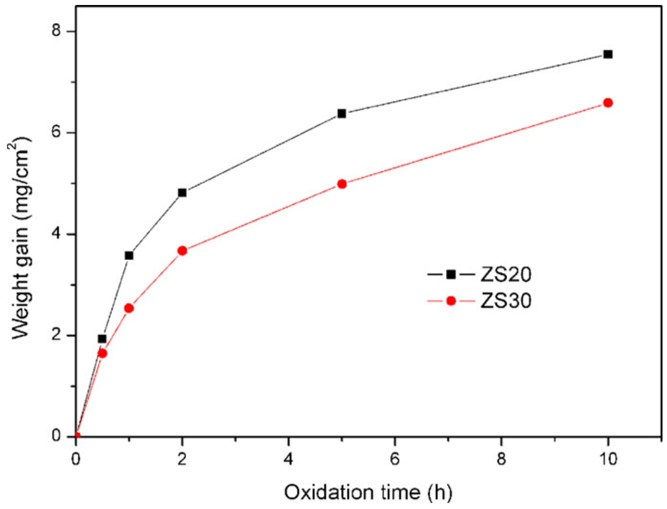

Fig. 2. The weight gain versus of oxidation time at 1500 °C for ZS20 and ZS30 ceramics.

22 μm respectively for ZS30 ceramics. The lower thickness of oxidized layer and mass gain both confirmed that the oxidation resistance of ZS30 ceramic was better than that of ZS20 ceramics.

In consideration of both mechanical properties and oxidation behavior, ZS30 with good oxidation resistance was selected as the outer layer for the ZrB_2–SiC laminated ceramic composites. ZS25 ceramics was used as the inner layer of the composites so that the residual compressive stress would appear in ZS30 layer due to the proper mismatch of thermal expansion coefficient of ZS25 ($6.175 \times 10^{-6}\,K^{-1}$) and ZS30 ($6.05 \times 10^{-6}\,K^{-1}$) while the tensile stress in ZS25 layer would not be too large to introduce cracks into ZS25 layer. Fig. 4 illustrated the schematic structure for the ZrB_2–SiC laminated ceramic composites. The thickness ratio (r) of outer layer (ZS30) and inner layer (ZS25) was introduced as one parameter. The physical properties of ZrB_2 and SiC were shown in Table 1.[24] The properties of ZS25 and ZS30 were calculated based on the rules of mixtures.

Fig. 4. Schematic illustrations of laminated structure.

Chartier[25] has proposed a simple formula to calculate the compressive stress:

$$\sigma^1 = \frac{nE_1E_2d_2(\alpha_2 - \alpha_1)\Delta T}{n(1-\nu_1)E_2d_2 + (n+1)(1-\nu_2)E_1d_1} \quad (4)$$

where $E_1, E_2, \alpha_1, \alpha_1, \nu_1, \nu_2, d_1$, and d_2 are the Young's modulus, thermal expansion coefficient, Poisson's ratio and layer thickness of outer layer and inner layer, respectively. ΔT and n are the difference in temperature between room and the sintering temperature and the amount of composite layers respectively.

Besides formula (4), finite element method (FEM) was also used to calculate the compressive stress in ZS30/ZS25/ZS30 laminated ceramic composites. The calculated results were shown in Table 2. Results indicated that the compressive stress increased with the decrease in thickness ratio (r). The results calculated by formula (4) were larger than that calculated by FEM.

The mechanical properties of as-prepared ZS30/ZS25/ZS30 laminated ceramic composites with different thickness ratio were shown in Table 3. The experimental results indicated that the surface compressive stress could effectively influence the flexural strength. The higher the surface compressive stress, the higher the flexural strength is. The fracture of ceramics basically initiated from the surface, therefore the strength of laminates should be equal to the sum of surface compressive stress and the strength of outer layer. For this reason, the surface

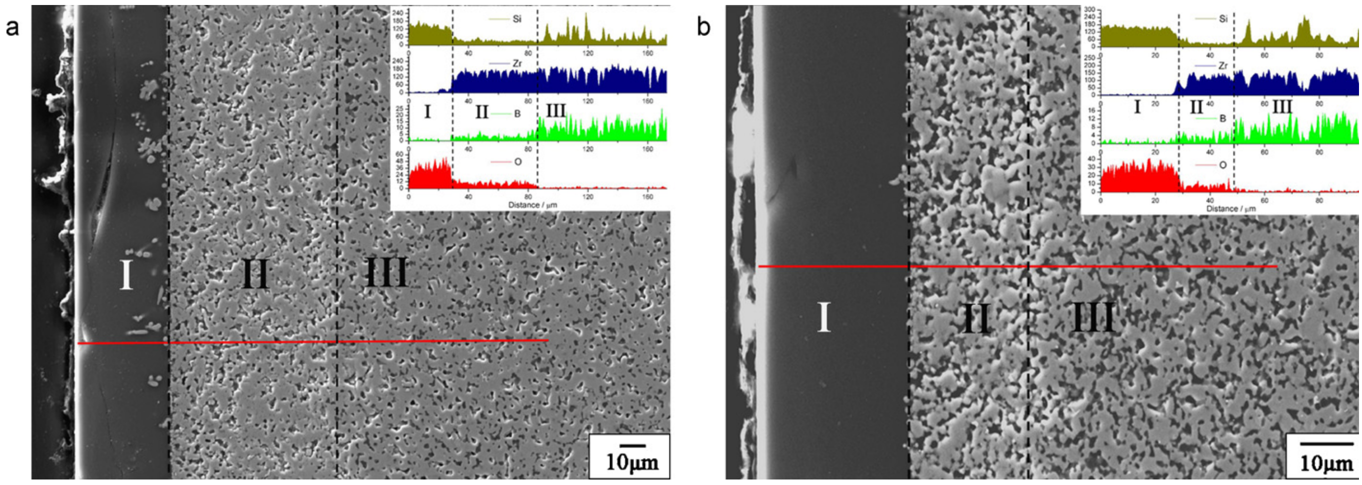

Fig. 3. Cross-sectional micrographs of (a) ZS20 and (b) ZS30 ceramics after oxidized at 1500 °C for 10 h.

Table 1
Properties of materials in laminated ceramics.

Materials Abbreviation	ZrB_2 Z	SiC S	ZrB_2 + 25 vol%SiC ZS25	ZrB_2 + 30 vol%SiC ZS30
Density (g/cm^3)	6.09	3.21	5.37	5.226
Elastic modulus (GPa)	489	430	473.516	470.484
Poisson ratio	0.14	0.16	0.145	0.146
Coefficient of thermal expansion (10^{-6} K^{-1})	6.8	4.3	6.175	6.05
Thermal conductivity (W/m K)	85	125	95	97
Specific heat (J/kg K)	422	668	458.654	466

Table 2
Surface compressive stress in ZS30/ZS25/ZS30 laminated ceramic composites.

r	Compressive stress calculated by formula (4) (MPa)	Compressive stress calculated by FEM (MPa)
1	56	37
0.5	78	55
0.2	102	79
0.1	114	92

Table 3
Mechanical properties of ZS30/ZS25/ZS30 laminated ceramic composites.

r	Flexural strength (MPa)	σ[a] (MPa)	Fracture toughness (MPa m$^{1/2}$)
1	562.6 ± 36.1	35.7	10.03 ± 1.26
0.5	580.1 ± 36.4	53.2	10.73 ± 0.91
0.2	596.3 ± 27.2	69.4	9.53 ± 0.93
0.1	624.1 ± 63.5	97.2	8.47 ± 1.14
ZS25	549.5 ± 88.6	–	5.54 ± 0.59
ZS30	526.9 ± 24.8	–	5.37 ± 1.06

[a] $\sigma = \sigma_{ZS30/ZS25/ZS30} - \sigma_{ZS30}$.

compressive stresses (σ) of ZS30/ZS25/ZS30 laminated ceramic composites were calculated based on the strength of laminar and ZS30 ceramic (see Table 3). It revealed that the calculated results by FEM showed a good agreement with that from testing.

The surface compressive stress could help to lower the stress field at the crack tip, which would contribute to the increase in fracture toughness.[25] Moreover, the stress state changed at the interface between inner layer and outer layer, which might lead to the crack deflection at the interface, as shown in Fig. 5. If the outer layer was too thin, the crack length after deflection was still short, which might contribute less to the increase in toughness. Therefore, the ZS30/ZS25/ZS30 laminates with a thickness ratio of 0.5 showed a higher fracture toughness of 10.73 MPa m$^{1/2}$, which was almost 2 times of that of ZS30 monolithic ceramics.

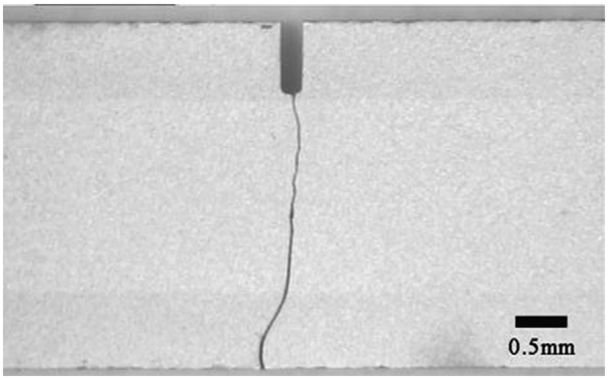

Fig. 5. The fractography of ZS30/ZS25/ZS30 laminated ceramic composites (r = 0.5).

4. Conclusions

Nearly fully densified ZrB_2–SiC ceramics were obtained by aqueous tape casting. Increase in SiC content from 20 vol% to 30 vol% led to the form of larger SiC agglomerates, which therefore resulted in a decrease in mechanical properties. ZS30 ceramics had lower oxidized layer thickness and weight gain than ZS20 ceramics after oxidized at 1500 °C for 10 h, so ZS30 layers were selected as the outer layer for preparing ZS30/ZS25/ZS30 laminated ceramic composites. The surface residual compressive stress was found to increase with the decrease of thickness ratio (r). Higher surface compressive stress resulted in higher flexural strength. The fracture toughness of ZS30/ZS25/ZS30 laminates reached to 10.73 MPa m$^{1/2}$ at the thickness ratio of 0.5, which was almost 2 times of that of ZS30 monolithic ceramics. Results showed that the mechanical properties could be tailored through the careful composition and structural design of the composites.

Acknowledgements

This work was supported by the National Natural Science Foundation of China (No. 50772128), the Shanghai Science and Technology Committee (No. 07DJ14001) and the State Key Laboratory of High Performance Ceramics and Superfine Microstructures.

References

1. Fahrenholtz WG, Hilmas GE, Talmy IG, Zaykoski JA. Refractory diborides of zirconium and hafnium. *J Am Ceram Soc* 2007;**90**(5):1347–64.
2. Levine SR, Opila EJ, Halbig MC, Kiser JD, Singh M, Salem JA. Evaluation of ultra high temperature ceramics for aeropropulsion use. *J Eur Ceram Soc* 2002;**22**(14–15):2757–67.
3. Opeka MM, Talmy IG, Zaykoski JA. Oxidation-based materials selection for 2000 °C + hypersonic aerosurfaces: theoretical considerations and historical experience. *J Mater Sci* 2004;**39**(19):5887–904.
4. Van Wie DM, Drewry Jr DG, King DE, Hudson CM. The hypersonic environment: required operating conditions and design challenges. *J Mater Sci* 2004;**9**(19):5915–24.
5. Morz C. Zirconium diboride. *Am Ceram Soc Bull* 1994;**73**(6):141–2.
6. Culter RA. Engineering properties of borides. In: Schneider Jr SJ, editor. *Ceramics and glasses, engineered materials handbook*, vol. 4. Materials Park, OH: ASM International; 1991. p. 787–811.
7. Upadhya K, Yang JM, Hoffman WP. Materials for ultrahigh temperature structural applications. *Am Ceram Soc Bull* 1997;**76**(12):51–6.
8. Hwang SS, Vasiliew AL, Padture NP. Improved processing and oxidation-resistance of ZrB_2 ultra-high temperature ceramics containing SiC nanodispersoids. *Mater Sci Eng A* 2007;**464**:216–24.
9. Monteverde F. Beneficial effects of an ultra-fine α-SiC incorporation on the sinterability and mechanical properties of ZrB_2. *Appl Phys A* 2006;**82**:329–37.
10. Monteverde F, Bellosi A. Development and characterization of metal-diboride-based composites toughened with ultra-fine SiC particulates. *Solid State Sci* 2005;**7**:622–30.
11. Zhu S, Fahrenholtz WG, Hilmas GE. Influence of silicon carbide particle size on the microstructure and mechanical properties of zirconium diboride-silicon carbide ceramics. *J Eur Ceram Soc* 2007;**27**:2077–83.
12. Han J, Hu P, Zhang X, Meng S. Oxidation behavior of zirconium diboride-silicon carbide at 1800 °C. *Scripta Mater* 2007;**57**:825–8.
13. Ni D, Zhang G, Kan Y, Sakka Y. Highly textured ZrB_2-based ultrahigh temperature ceramics via strong magnetic field alignment. *Scripta Mater* 2009;**60**:615–8.
14. Clegg WJ, Kendall K, Alford NMcN, Button TW, Birchall JD. A simple way to make tough ceramics. *Nature* 1990;**357**:455–7.
15. Vandeperre LJ, Kristoffersson A, Carlström E, Clegg WJ. Thermal shock of layered ceramic structures with crack-deflecting interfaces. *J Am Ceram Soc* 2001;**84**(1):104–10.
16. Lü ZH, Jiang DL, Zhang JX, Lin Q. Processing and properties of ZrB_2–SiC composites obtained by aqueous tape casting process. *Ceram Int* 2011;**37**:293–301.
17. Lü ZH, Jiang DL, Zhang JX, Lin Q. Aqueous tape casting of zirconium diboride. *J Am Ceram Soc* 2009;**92**(10):2212–7.
18. Chamberlain AL, Fahrenholtz WG, Hilmas GE, Ellerby DT. High strength zirconium diboride-based ceramics. *J Am Ceram Soc* 2004;**87**(6): 1170–2.
19. Rezaie A, Fahrenholtz WG, Hilmas GE. Effect of hot pressing time and temperature on the microstructure and mechanical properties of ZrB_2–SiC. *J Mater Sci* 2007;**42**:2735–44.
20. Zhu S, Fahrenholtz WG, Hilmas GE. Influence of silicon carbide particle size on the microstructure and mechanical properties of zirconium diboride–silicon carbide ceramics. *J Eur Ceram Soc* 2007;**27**:2077–83.
21. Zhang SC, Hilmas GE, Fahrenholtz WG. Pressureless sintering of ZrB_2–SiC ceramics. *J Am Ceram Soc* 2008;**91**(1):26–32.
22. Fahrenholtz WG. The ZrB_2 volatility diagram. *J Am Ceram Soc* 2005;**88**(12):3509–15.
23. Rezaie A, Fahrenholtz WG, Hilmas GE. Evolution of structure during the oxidation of zirconium diboride-silicon carbide in air up to 1500 °C. *J Eur Ceram Soc* 2007;**27**:2495–501.
24. Zimmermann JW, Hilmas GE, Fahrenholtz WG. Thermophysical properties of ZrB_2 and ZrB_2–SiC ceramics. *J Am Ceram Soc* 2008;**91**(5):1405–11.
25. Chartier T, Merle D, Besson J. Laminar ceramic composites. *J Eur Ceram Soc* 1995;**15**:101–7.